Fish and Shellfish Immunology 87 (2019) 460–469

Contents lists available at ScienceDirect

Fish and Shellfish Immunology

journal homepage: www.elsevier.com/locate/fsi

Full length article

# B52 promotes alternative splicing of *Dscam* in Chinese mitten crab, *Eriocheir sinensis*

Zhi-Cheng Wan[a,1], Dan Li[a,1], Xue-Jie Li[a], You-Ting Zhu[a], Tian-Heng Gao[b], Wei-Wei Li[a,*], Qun Wang[a,**]

[a] State Key Laboratory of Estuarine and Coastal Research, Laboratory of Invertebrate Immunological Defense and Reproductive Biology, School of Life Sciences, East China Normal University, Shanghai, China
[b] Institute of Marine Biology, College of Oceanography, Hohai University, Nanjing, Jiangsu, China

ARTICLE INFO

*Keywords:*
*Eriocheir sinensis*
Serine/arginine-rich protein B52
Alternative splicing activator
Dscam
Alternative splicing
mRNA maturation
PAMPs

ABSTRACT

B52 is a member of the classical serine/arginine (SR)-rich proteins, which are phylogenetically conserved and play significant roles in mRNA maturation, including alternative splicing. In the present study, the docking site, selector sequences and locus control region of the Chinese mitten crab (*Eriocheir sinensis*) Down syndrome cell adhesion molecule (*EsDscam*) were identified. Alternative splicing of *Dscam* is essential to generate different isoforms. We also isolated and characterised the B52 gene from *E. sinensis* (*EsB52*). The 876 bp open reading frame of *EsB52* encodes a 291 amino acid residue polypeptide, and *EsB52* has two RNA recognition motifs (RRMs) at the N-terminus and an arginine/serine-rich domain at the C-terminus. Each RRM contains two degenerate short submotifs, RNP-1 and RNP2. Analysis of tissue distribution revealed that *EsB52* mRNA expression was widespread in all tested tissues, and especially high in brain and hemocytes. In hemocytes, *EsB52* was upregulated significantly after stimulation with pathogen-associated molecular patterns and bacteria. Furthermore, *EsB52* RNAi decreased the number of Ig7 inclusion in mRNA rather than Ig2 or Ig3. Taken together, these findings suggest that *EsB52* acts as an alternative splicing activator of *EsDscam*.

## 1. Introduction

The Down syndrome cell adhesion molecule (*Dscam*) belongs to a family of cell membrane molecules involved in differentiation of the nervous system, and in the specific recognition and binding activity of innate immune reactions [1–3]. *Dscam* has been recently referred to as hypervariable (*Dscam-hv*) due to the large number of possible isoforms [4]. The most striking characteristic of *Dscam-hv* is alternative splicing [5–8], which can generate 38,016 different isoforms through mutually exclusive splicing of the four cassette exon clusters in *Drosophilla melanogaster* [9]. There are several variable regions in the extracellular region (Ig2, Ig3 and Ig7) of Arthropod *Dscam*, as well as a transmembrane domain and a cytoplasmic tail [10,11]. Alternative splicing is an ancient and widespread mechanism used by eukaryotes to expand protein diversity and regulate gene expression, which may contribute to subsequent functional differentiation [12–14]. Up to 95% of primary transcripts in humans are estimated to undergo alternative splicing [15]. Mutually exclusive splicing is strictly regulated by alternative splicing in which the splicing machinery must choose one of two or more candidate exons to include in each mRNA isoform, which are subsequently translated into different proteins with a constant non-alternatively-spliced region, and variable alternative splicing regions [16].

The most attractive model for mutually exclusive splicing involves competition among RNA secondary structures [17]. This mechanism was discovered in *Dscam-hv* within the exon 6 cluster, which encodes Ig3 in *Drosophila* [7]. The exon 6 cluster contains two conserved and complementary elements; a docking site, which is located in the intron downstream of constitutive exon 5, and selector sequences, which are located upstream of each of the 48 exon 6 variants. The docking site is partially complementary to each of the selector sequences, partially complementary features can bind only one selector sequence at the docking site during *Dscam-hv* mRNA maturation, and s similar structural arrangement is present in *Drosophila Dscam* exon clusters for Ig2 and Ig7 [18].

However, the secondary structure of RNA alone cannot explain

* Corresponding author.
** Corresponding author.
*E-mail addresses:* wwli@bio.ecnu.edu.cn (W.-W. Li), qwang@bio.ecnu.edu.cn (Q. Wang).
[1] These authors contributed equally to this work.

https://doi.org/10.1016/j.fsi.2019.01.027
Received 12 July 2018; Received in revised form 15 January 2019; Accepted 21 January 2019
Available online 24 January 2019

**Table 1**
Sequences of primers used for *EsB52* analysis.

| Primer name and purpose | Sequence (5′-3′) |
|---|---|
| **cDNA cloning** | |
| *EsB52*-5′ RACE | CCTGTACTTGTGGGCGTCGGC |
| *EsB52*-3′ RACE | CGGCTTTGGCTTCGTGGAGTT |
| **Real-time quantitative PCR** | |
| β-actin qF | GCATCCACGAGACCACTTACA |
| β-actin qR | CTCCTGCTTGCTGATCCACATC |
| B52 qF | ACCGTTTCTTCCGCTCCTAC |
| B52 qR | GCTCCTTTCCGTTCATCTCATAC |
| **RNA interference** | |
| si*EsB52* F | GGGACAUCGUCAUCAAGAATT |
| si*EsB52* R | UUCUUGAUGACGAUGUCCCTT |
| **Hypervariable region amplification** | |
| Ig2-F | GCACGCTGATGTTTCCACCTTT |
| Ig2-R | GGTATTTGCCATCTGCGGGAC |
| Ig3-F | GCACGCTGATGTTTCCACCTTT |
| Ig3-R | GCTCAAAGCGTCCTCCAAGT |
| Ig7-F | ATGATTGTCCACTGCCCTGT |
| Ig7-R | CAATCTGAAGGGTGCCATC |
| **Clone sequencing** | |
| 23-Mer | CGACTCACTATAGGGAGAGCGGC |
| 24-Mer | AAGAACATCGATTTTCCATGGCAG |

which exon is selected by the interaction between docking sites and selector sequences, hence we must identify proteins that regulate alternative splicing of *Dscam-hv*. Based on this mechanism, there are two types of antagonistic and conserved alternative splicing regulators; the serine/arginine (SR)-rich protein family, and the heterogeneous nuclear ribonucleoprotein (hnRNP) family. During pre-mRNA maturation, these families play opposite roles in alternative splicing. SR proteins act as splicing activators and bind to exonic splicing enhancer (ESE) elements and recruit core splicing machinery proteins to the splicing site to prevent exon skipping, thereby ensuring ESE-containing exons in spliced mRNA [19]. By contrast, hnRNP proteins act as splicing repressors and bind to exonic splicing silencer (ESS) elements. This prevents small nuclear ribonucleoprotein particles (snRNPs) from binding to the splicing site, excluding the alternative exon from the spliced mRNA [20].

Two RNAi screening studies revealed that some splicing regulators might have roles in *Dscam-hv* alternative splicing in *Drosophila* S2 cells [21,22]. We proposed that *hrp36* binds to most if not all exon 6 variants to represses their inclusion when a selector sequence interacts with the docking site. This causes *hrp36* to bind the downstream exon to prevent its selection. *Hrp36* competes with SR-rich proteins for binding to exon 6 variants. In the absence of *hrp36*, SR-rich proteins can bind to all exon

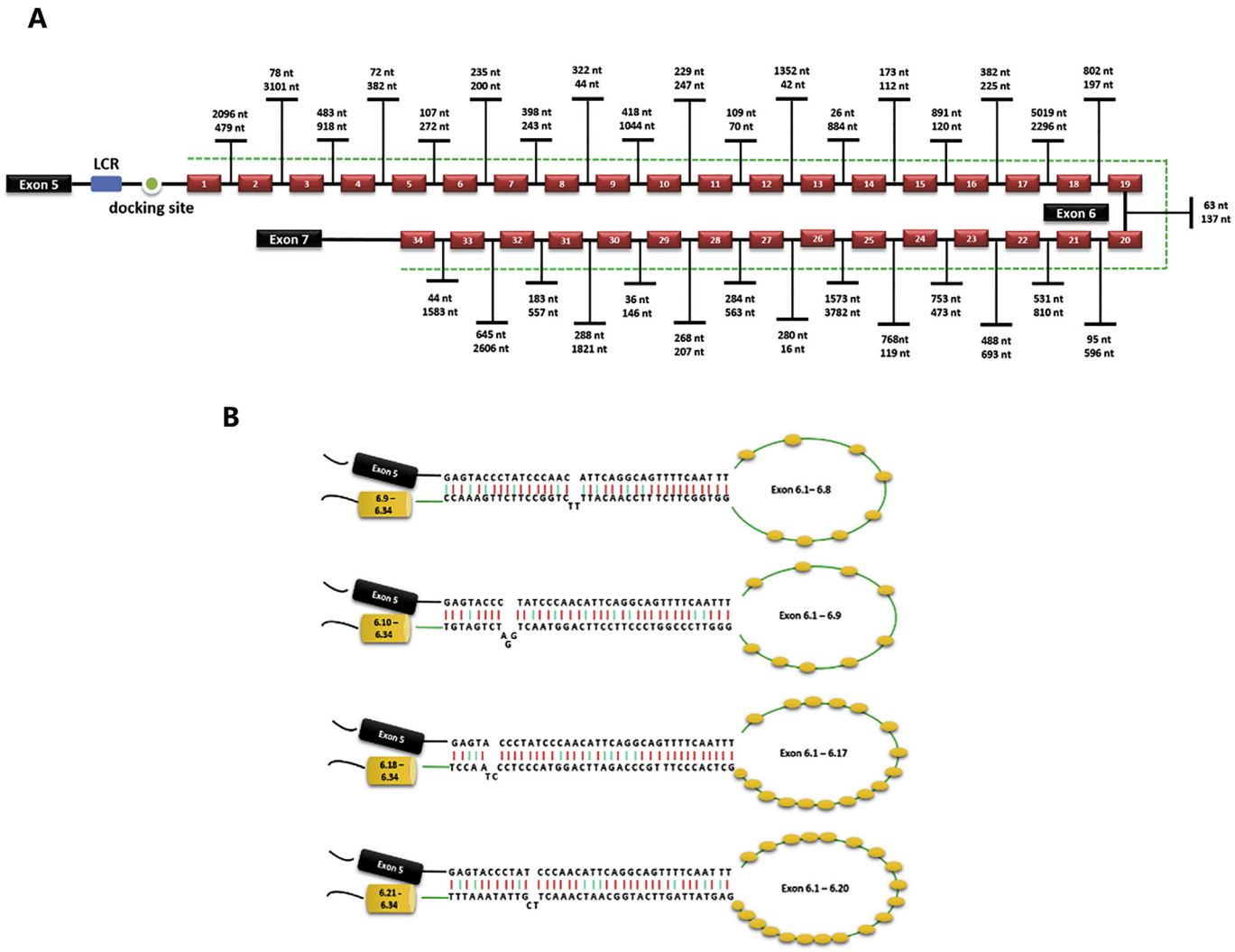


**Fig. 1. The docking site and selector sequences of *EsDscam-hv*.** (A) The location of the docking site, selector sequences, and the locus control region (LCR) in the exon 6 cluster. Selector sequences are located in introns between each small exon. The upper numbers indicate the length from the selector sequence to the previous exon, and the lower numbers indicate the length from selector sequence to the next exon. (B) RNA secondary structures of the docking site with exon 6.8, 6.9, 6.17, and 6.20 selector sequences from *Eriocheir sinensis*. These examples demonstrate that the docking site engages in base-pairing interactions with the selector sequences.

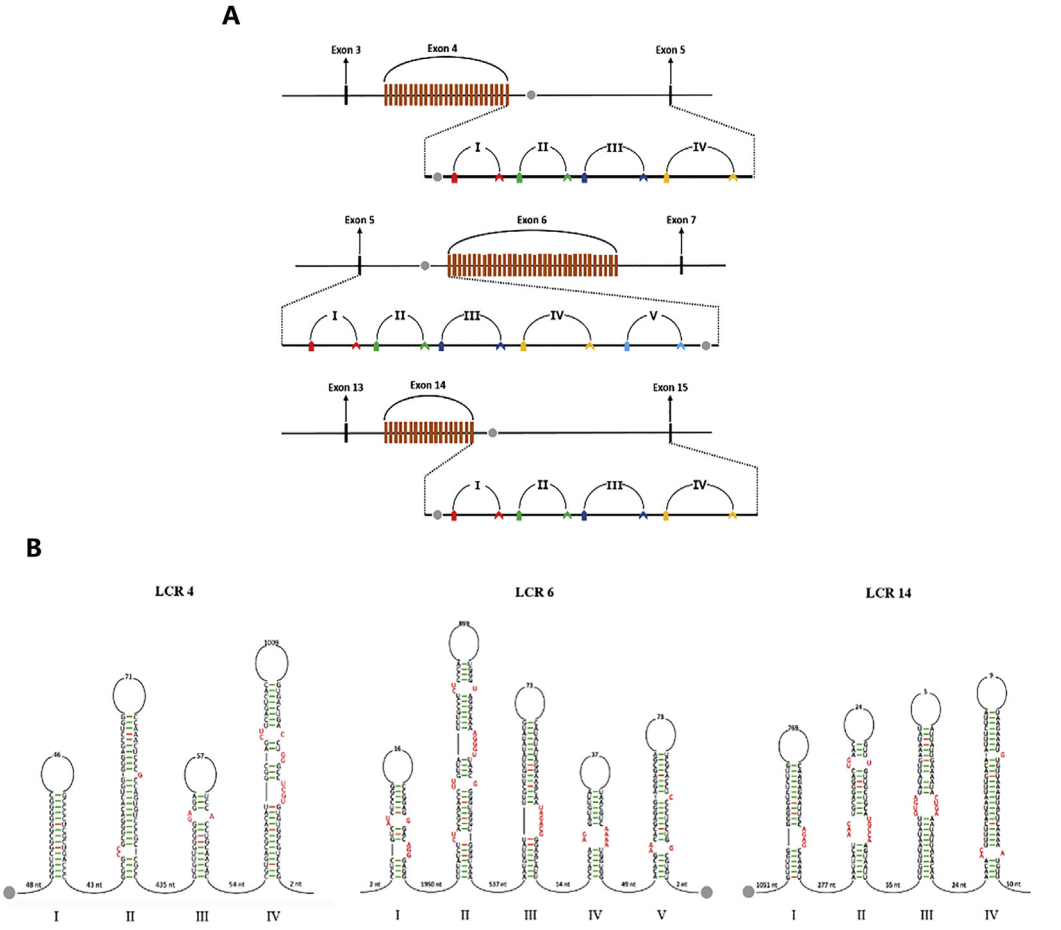


**Fig. 2. The locus control region (LCR) of *EsDscam-hv*.** (A) The location and number of LCRs in exons 4, 6 and 14 in *E. sinensis*. (B) The predicted tetramer architecture and secondary structure of the LCR in *E. sinensis* pre-mRNA.

6 variants and enhance the abundance of exon 6 isoforms [21]. These include the B52 protein that activates exon inclusion and possesses two RNA recognition motifs (RRMs) in the N-terminus, and an RS-rich domain at the C-terminus [23]. Another silencing study in *Litopeneaus vannamei* revealed that B52 acts as a splicing activator that regulates alternative splicing of *Dscam-hv* [24]. However, it is not clear exactly what role B52 plays in the alternative splicing of *Dscam-hv* in Chinese mitten crab (*Eriocheir sinensis*).

*Dscam-hv* molecules are widely expressed in the nervous system, and their functions are critical in neural circuit formation [25]. Transcripts of fly *Dscam-hv* have been detected in components of the insect immune system, including fat body cells and hemocytes [1]. Moreover, depletion of *Dscam-hv* impairs the ability of *D. melanogaster* hemocytes to phagocytose bacteria [11]. These phenomena, and the presence of a large number of different isoforms, provide evidence of the potential roles of *Dscam-hv*, and explain the almost endless possibilities of its immunological functions. *Dscam-hv* is particularly interesting due to its extreme encoding versatility and molecular diversity, and also because the nervous and immune systems may exert different selection pressures on this gene.

In the present study, we analysed the alternative splicing mechanism of *Dscam-hv* in *E.* sinensis to build on the results of our previous study [26]. The findings provide insights into the mechanism of alternative splicing that results in the high molecular diversity of *Dscam-hv*. We also cloned and characterised the full-length cDNA sequence of *EsB52*, and measured its expression in different tissues, and following stimulation with bacteria and pathogen-associated molecular patterns (PAMPS). Finally, we performed RNA interference *in vitro* to investigate the role of *B52* in alternative splicing of *EsDscam*.

## 2. Materials and methods

### 2.1. Experimental animals

Healthy adult Chinese mitten crabs (n = 150; 100 ± 20 g wet weight) were collected from the Xin'An Market in Shanghai, China, and maintained in filtered and aerated fresh water for 1 week under constant temperature (20–25 °C).

### 2.2. Sequence alignment and secondary structure prediction

The full-length mRNA sequence of *EsDscam* was obtained from our previous study [26]. To identify the docking site of *EsDscam-hv*, alignment of *Dscam* genes from *Drosophila* species (*D. melanogaster*, *D. simulans*, *D. yakuba*, *D. erecta*, *D. ananassae*, *D. pseudoobscura*, *D. persimilis*, *D. willistoni*, *D. mojavensis*, *D. virilis*, and *D. grimshawi*) was performed using Multi-PipMaker (http://pipmaker.bx.psu.edu/cgi-bin/multipipmaker) [27]. Alignments of specific regions between species were further refined using the ClustalW program (http://www.ebi.ac.uk/Tools/msa/clustalw2/), as were alignments of the selector sequences. Consensus sequences of selector sequences were derived using WebLogo (http://weblogo.berkeley.edu/) [28], and selector sequences complementary to the docking site were identified.

Intronic RNA secondary structures were predicted using the Mfold program [29], which included interactions between docking sites and selector sequences, and the locus control region (LCR).

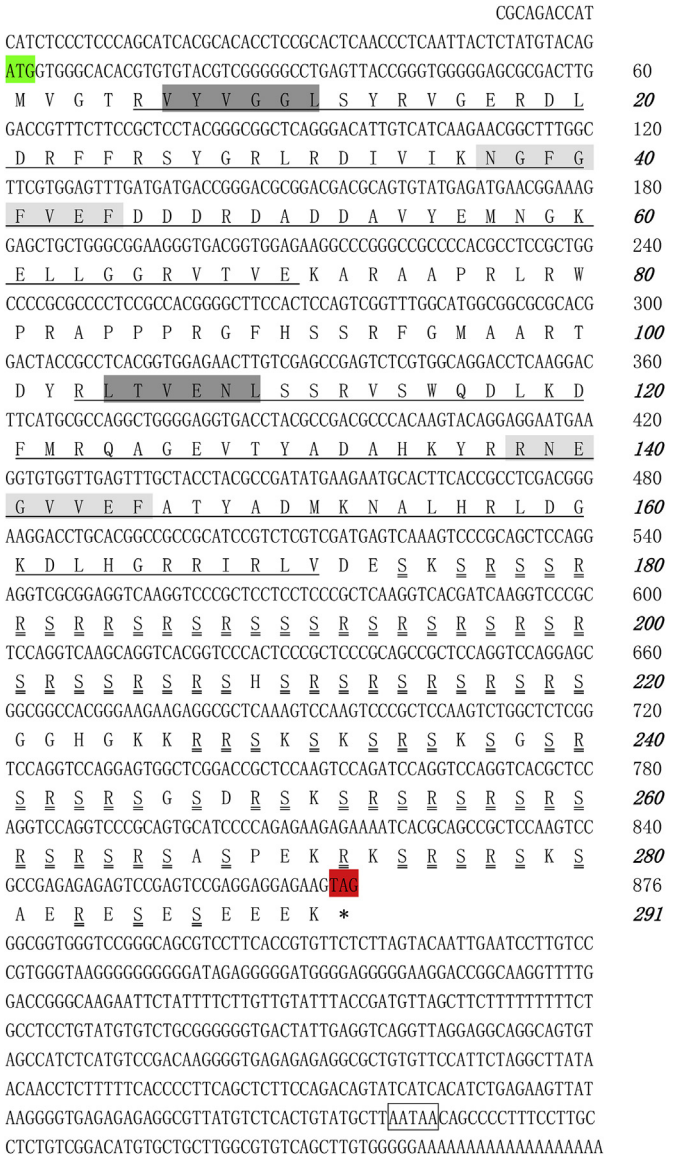


**Fig. 3. Nucleotide and deduced amino acid sequences of *EsB52*.** Deduced *EsB52* amino acid sequences are shown below cDNA sequences. The two RNA recognition motifs (RRM) are underlined, and the RNA binding domain RNP-1 is shaded light grey, while RNP-2 is shaded dark grey. Each arginine (R) and serine (S) in the RS-rich domain is double-underlined. Start codons (ATG) are shaded green, stop codons (TAG) are shaded red, and the polyadenylation site (AATAA) is boxed. (For interpretation of the references to colour in this figure legend, the reader is referred to the Web version of this article.)

### 2.3. Sample collection and animal immune stimulation

Crabs were placed in an ice bath for 3–5 min until slightly anesthetised, and hemolymph was drawn from the hemocoel of the arthrodial membrane of the last pair of walking legs using a syringe (~5.0 mL per crab) with an equal volume of anticoagulant solution (0.1 M glucose, 30 mM citrate, 26 mM citric acid, 0.14 M NaCl and 10 mM ethylenediaminetetraacetic acid) [30]. Hemolymph was centrifuged at 800 × *g* and 4 °C to isolate hemocytes. Other tissues (gill, muscle, stomach, intestine, liver and brain) were collected, snap-frozen in liquid nitrogen, and stored at −80 °C for subsequent analysis. For cloning and expression analyses, identical tissue samples from 10 crabs were pooled and ground with a mortar and pestle prior to extraction.

For stimulation by bacteria and PAMPs, more than 100 crabs were divided equally into five groups (sex ratio = 1:1). Two experimental groups were injected in the arthrodial membrane of the last pair of walking legs with 100 μL of lipopolysaccharide (LPS) from *E. coli* (Sigma-Aldrich, St. Louis, MO, USA) and 100 μL of peptidoglycan (PG) from *Staphylococcus aureus* (Sigma-Aldrich) resuspended in 500 μg/mL phosphate-buffered saline (PBS; 137 mM NaCl, 2.7 mM KCl, 10 mM Na2HPO4, and 2 mM KH2PO4, pH 7.4). For bacterial stimulation, *Vibrio parahaemolyticus* (BYK00036) and *S. aureus* (BYK0113) were obtained from the National Pathogen Collection Center for Aquatic Animals (Shanghai Ocean University, Shanghai, China). Strains were cultured overnight in Luria-Bertani (LB) medium and collected by centrifugation at 5000 × *g* for 5 min. After removing the supernatant, strains were washed two or three times with sterile PBS, resuspended in fresh PBS, and plated for colony counting. The other two experimental groups were injected with 100 μL of bacterial suspension ($1 \times 10^6$ colony-forming units/mL) of *V. parahemolyticus* or *S. aureus*. In the control group, crabs were injected with 100 μL of PBS (pH 7.4. More than five crabs were randomly selected at time 0 (blank controls), and at each time interval (12, 24, 36 and 48 h post-injection). Hemocytes were collected according to the methods above, and stored at −80 °C for subsequent analysis.

### 2.4. Total RNA extraction and first-strand cDNA synthesis

Using TRIzol reagent (Invitrogen, Carlsbad, CA, USA), total RNA was extracted from *E. sinensis* tissues according to the manufacturer's protocol. The concentration and purity of total RNA were estimated using a NanoDrop 2000 spectrophotometer (Thermo Scientific, Waltham, MA, USA) and agarose gel electrophoresis, respectively. The SMARTer RACE cDNA Amplification Kit (Clontech, Mountain View, CA, USA) was used to reverse-transcribe total RNA (5 μg) from hemocytes into full-length cDNA. For quantitative real-time PCR (RT-qPCR) analysis, total RNA (1000 ng) was reverse-transcribed using a PrimeScript RT Reagent Kit with gDNA Eraser (TaKaRa, Shiga, Japan).

### 2.5. Cloning of the full-length EsB52 cDNA

A partial *EsB52* cDNA sequence was obtained from the hemocyte cDNA library (unpublished) and extended by 3′ and 5′ rapid amplification of cDNA ends (RACE) using a SMARTer RACE cDNA Amplification Kit (Clontech) according to the manufacturer's protocol. Gene-specific primers (Table 1) were designed based on the original expressed sequence tag (EST) sequence, and 3′ and 5′ RACE were performed at 94 °C for 4 min, followed by 35 cycles at 94 °C for 30 s, 62 °C for 30 s, and 72 °C for 90 s, and a final extension at 72 °C for 10 min. PCR products were purified and inserted into the pZeroBack/Blunt Vector (Tiangen, China) and transformed into competent *E. coli* TOP10 cells. Positive clones containing inserts were sequenced in both directions using 23-mer and 24-mer primers (Table 1).

### 2.6. Analysis of the full-length EsB52 cDNA

The full-length *EsB52* cDNA and predicted amino acid sequences were compared with sequences from other representative vertebrates and invertebrates in the National Center for Biotechnology Information (NCBI) database using the BLASTX online search tool (http://www.ncbi.nlm.nih.gov/). The structure and functional domains of *EsB52* were predicted using ExPASy (http://prosite.expasy.org/prosite.html/) and SMART (http://smart.embl-heidelberg.de/). Multiple sequence alignment was performed using the ClustalX 2.0 program and DNAMAN software, and phylogenetic trees were constructed with MEGA6 software.

### 2.7. Real-time quantitative PCR analysis of EsB52

Quantitative RT-PCR was performed using SYBR Premix Ex TaqTM (TaKaRa) with an *EsB52* gene-specific primer pair (Table 1), resulting in

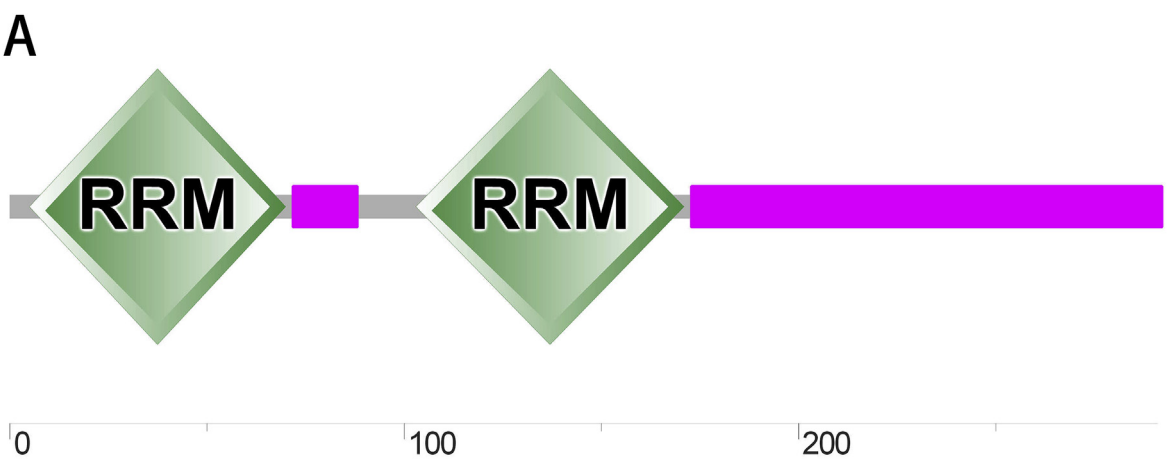


B

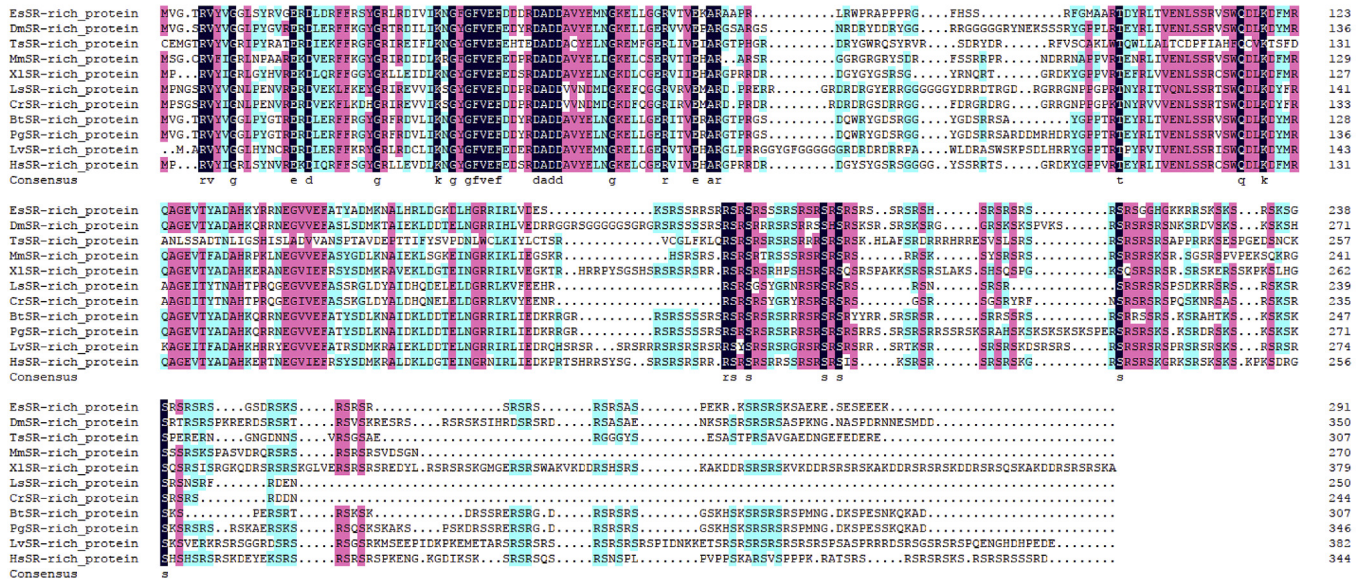


**Fig. 4. Schematic view of the structure of the *EsB52* protein and comparison of *EsB52* with its closest orthologs.** (A) Domain analysis of the putative *EsB52* protein using SMART. The two RRM domains are shown. (B) Sequences and accession numbers of proteins used for alignment are as follows: *Drosophila melanogaster* CAA41556.1, *Trichinella spiralis* KRY28632.1, *Mus musculus* NP_001334345.1, *Xenopus laevis* NP_001079647.1, *Lepeophtheirus salmonis* ACO12341.1, *Caligus rogercresseyi* ACO10556.1, *Bombus terrestris* XP_012169705.1, *Pseudomyrmex gracilis* XP_020293235.1, *Homo sapiens* NP_006266.2, *Litopenaeus vannamei* [24]. Identical (black) and similar (red or blue) residues are indicated. (For interpretation of the references to colour in this figure legend, the reader is referred to the Web version of this article.)

a 123 bp amplicon using a CFX96 instrument (Bio-Rad, Hercules, CA, USA). Reactions were performed at 95 °C for 30 s, followed by 40 cycles at 95 °C for 5 s and 60 °C for 30 s. The *β-actin* gene in was used as an internal control, with the exception of an alternate gene-specific primer pair (Table 1) as described above, designed based on a cloned *E. sinensis* β-*actin* cDNA fragment to produce a 276 bp amplicon. All qRT-PCR experiments were performed in triplicate using independently extracted RNA. For both tissue tropism and immune challenge transcription assays, PCR templates were obtained as described above in section 2.2. Data from qRT-PCR experiments were analysed using CFX Manager software, and the relative expression level of *EsB52* was calculated using the $2^{-\Delta\Delta Ct}$ comparative CT method [31].

### 2.8. In vitro RNAi

RNAi experiments were performed using siRNAs targeting *EsSB52* or *GFP* as a control (Table 1), which were obtained from GenePharma (GenePharma, Shanghai, China). A 5 μg sample of siRNA was transfected into cultured *E. sinensis* primary hemocytes for 24 h using siRNA-Mate reagent (GenePharma) according to the manufacturer's instructions (sterile PBS was used as a control). *E. sinensis* primary hemocytes were cultured was according to the method reported in our previous study [32]. Total RNA was extracted and reverse-transcribed to analyse the efficiency of RNAi silencing.

### 2.9. Amplification of EsDscam extracellular hypervariable regions in EsB52-silenced templates

Base on the full-length *EsDscam* mRNA sequence [26], we designed three pairs of primers (Table 1) to amplify the extracellular hypervariable regions (Ig2, Ig3 and Ig7) in *EsB52*-silenced samples. PCR experiments were performed using ExTaq Hot Start (TaKaRa) and

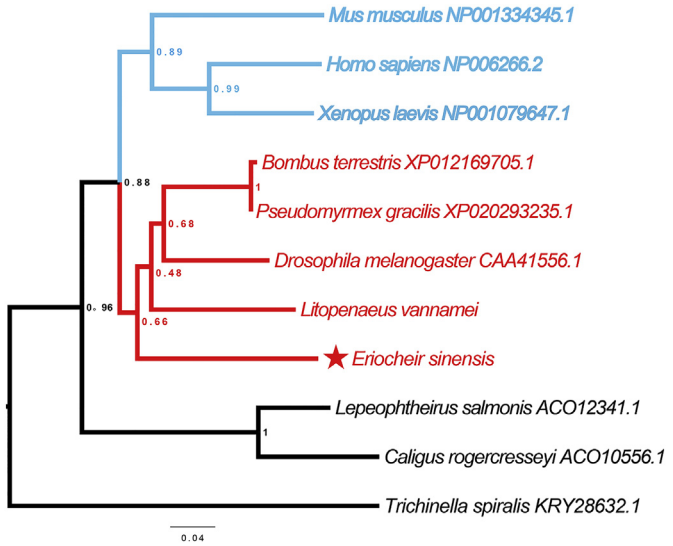


**Fig. 5. Neighbour-joining phylogenetic analysis of SR-rich proteins**. The phylogenetic tree was constructed by MEGA 6, and sequences and their accession numbers are shown on the graph. Numbers at branch nodes present bootstrap support (percentage) based on 3000 replications. The red triangle (★) indicates *EsB52*. Vertebrates (blue) and invertebrates (red and black) are indicated. (For interpretation of the references to colour in this figure legend, the reader is referred to the Web version of this article.)

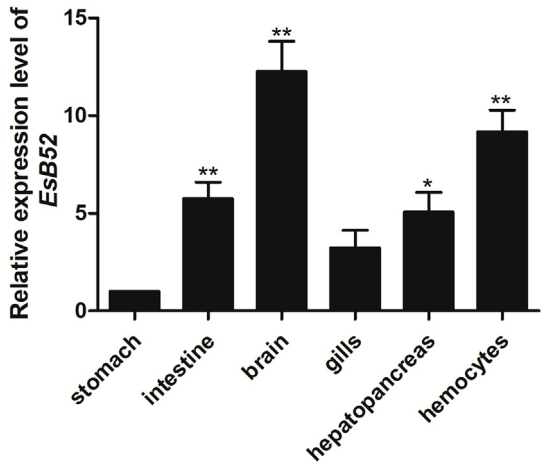


**Fig. 6. Tissue distribution of *EsB52*.** Expression of *EsB52* was examined in various tissues by real-time quantitative PCR. The *β-actin* gene of *E. sinensis* was used as an internal control. The assay was performed in triplicate, and asterisks indicate significant differences ($*p < 0.05$, $**p < 0.01$) in *EsB52* expression relative to levels in stomach.

templates were obtained s described above in section 2.7. Reactions were performed at 98 °C for 10 min, 94 °C for 30 s, followed by 35 cycles at 94 °C for 30 s, 56 °C for 30 s, and 72 °C for 90 s, and a final extension at 72 °C for 10 min. PCR products were cloned into competent *E. coli* TOP10 cells according to the method escribed above in section 2.4, and 100 individual clones from three Ig domains were sequenced in both directions.

### 2.10. Statistical analysis

SPSS software (Ver. 16.0) was used for statistical analysis, and data are presented as mean ± standard error. Statistical significance was determined using one-way analysis of variance and Duncan's post-hoc multiple range tests. Significance was set at $p < 0.05$ (*) and $p < 0.01$ (**).

## 3. Results

### 3.1. RNA secondary structures of EsDscam-hv

Multiple sequence alignment of the *E. sinensis Dscam-hv* gene with orthologs from 16 insect species revealed a number of conserved intronic elements, the majority of which are located in the exon 6 cluster. The most highly conserved element in the entire *Dscam-hv* gene is located in the intron between the constitutive exon 5 and the first exon of the exon 6 cluster, and is referred to as the docking site (Fig. 1A). The docking site is ~40 bp in *E. sinensis* (Fig. 1B) and shares high identity with the 10 *Drosophila* species examined, but lower than the 90–100% identity among the 10 *Drosophila* species, possibly due to species differences and evolutionary pressure.

The second class of identified conserved elements are termed selector sequences. Initial selector sequences were identified as relatively conserved sequences in introns upstream of some of the exon 6 variants. For instance, the selector sequences upstream of *E. sinensis Dscam-hv* exons 6.9, 6.10, 6.18 and 6.21 share high sequence identity and a highly complementary docking site (Fig. 1B). However, this was not the case for all, since some other selector sequences share comparable low identities between themselves (Supplementary Fig. S1). By searching the remaining exon 6 cluster for sequences that are similar, but not identical, to the initially identified selector sequences, a potential selector sequence was identified upstream of each exon 6 variant.

Strikingly, the central region of the *E. sinensis Dscam-hv* consensus selector sequence is complementary to the docking site consensus sequence, similar to *D. melanogaster*. All selector sequences overlap with one another to some extent; therefore, the docking site is predicted to interact with only one selector sequence at a time. Thus, docking site-selector sequence interactions presumably simultaneously juxtapose exon 5 with the exon 6 variant that is to be included, and this could explain how alternative splicing of these exons is mutually exclusive.

The LCR could activate the hypervariable exon cluster and specifically allow for the selection of only one exon splice variant in combination with competing RNA structures between docking site-selector sequences (Fig. 2A). We found four LCRs between the exon 4 cluster and exon 5, five between exon 5 and the exon 6 cluster, and four between the exon 14 cluster and exon 15 (Fig. 2B).

### 3.2. Characterisation of EsB52

The obtained full-length *E. sinensis Dscam* cDNA has been submitted to GenBank under accession number MF582352, and contain a 5′-untranslated region (UTR), and open reading frame (ORF), and a 3′ UTR. The ORF is 876 bp and encodes a 291 amino acid residue protein. *EsB52* contains two copies of an RRM, located between amino acids (aa) 5–70 and 103–171 in the N-terminal region, and an RS domain in the C-terminal region. Each RRM contains two degenerate short submotifs, RNP-1 and RNP2 (Fig. 3). *EsB52* shares a typical domain architecture with other *B52* orthologs according to analysis of the deduced amino acid sequence using ExPASy and SMART, and a signal peptide was not found (Fig. 4A). Multiple sequence alignment revealed relatively high conservation in the SR-rich protein family (Fig. 4B).

A phylogenetic tree was constructed based on analysis of *EsB52* and protein sequences of representative invertebrate and vertebrate orthologs. The tree contains two distinct clades distinguishing invertebrate SR-rich proteins (red) from vertebrate sequences (blue; Fig. 5).

### 3.3. Tissue distribution of EsB52

RT-PCR with *β-actin* as an internal control was performed to analyse the relative expression levels of *EsB52* in different tissues (stomach, intestine, brain, gill, hepatopancreas and hemocytes; $*p < 0.05$, $**p < 0.01$). *EsB52* mRNA expression was observed in all tested tissues, and was especially high in brain and hemocytes (Fig. 6).

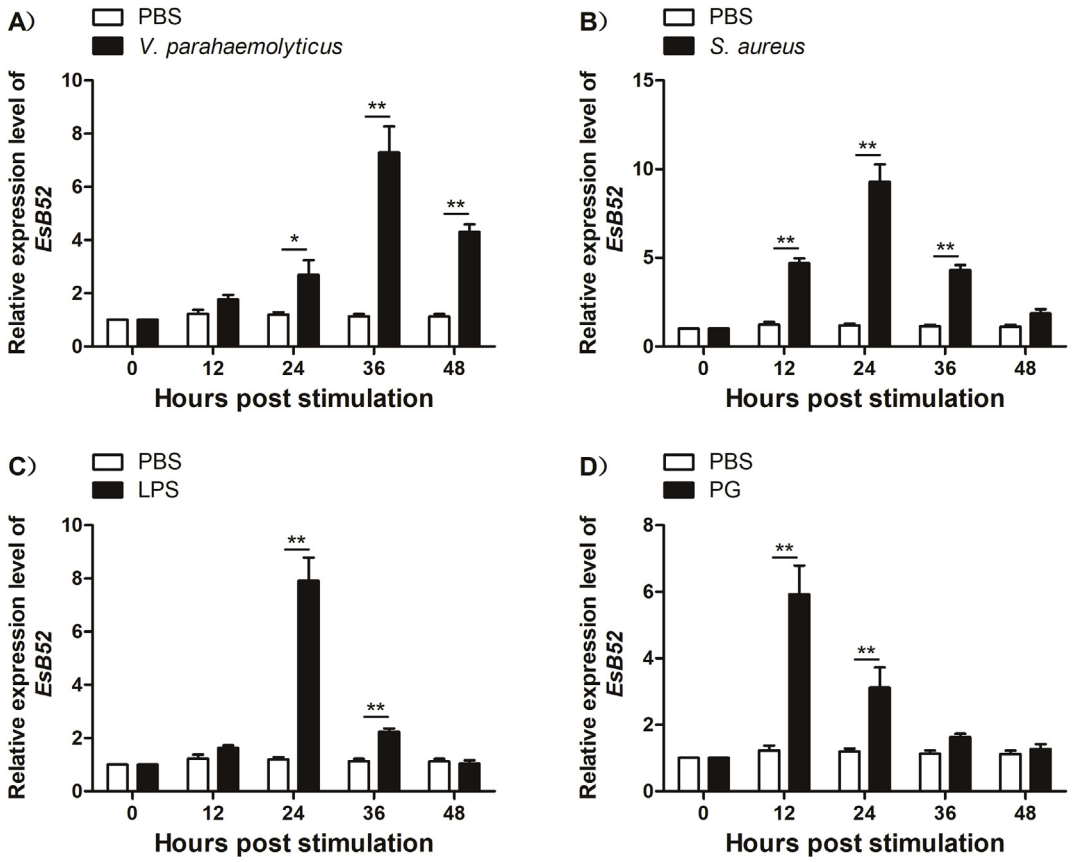


**Fig. 7. *EsB52* mRNA expression levels are enhanced following stimulation with PAMPs and bacteria.** *EsB52* expression was significantly enhanced compared with the control (white bars) as follows: (A) 24 h (*$p < 0.05$), 36 h and 48 h (**$p < 0.01$) after *Vibrio parahaemolyticus* stimulation; (B) 12 h, 24 h and 36 h (**$p < 0.01$) after *Staphylococcus aureus* stimulation; (C) 24 h and 36 h (**$p < 0.01$) after lipopolysaccharide (LPS) stimulation; (D) 12 h and 24 h (**$p < 0.01$) after peptidoglycan (PG) stimulation.

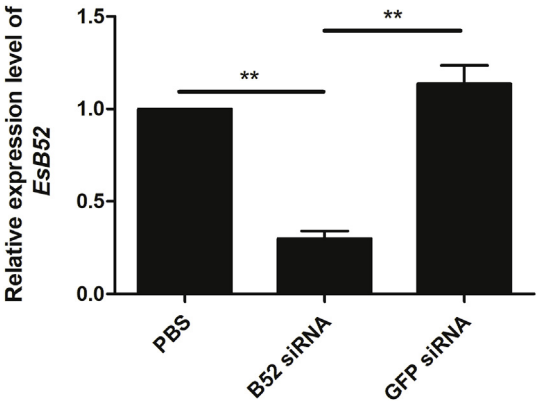


**Fig. 8. Efficiency of RNAi silencing of *EsB52 in vitro*.** A 5 μg sample of siRNA targeting *EsB52* (experimental group) was transfected into cultured *E. sinensis* primary hemocytes for 24 h, while control groups were treated with PBS and si*GFP* RNAi. qRT-PCR was performed to analyse *EsB52* mRNA expression levels (*β-actin* served and an internal control). Statistical significance is indicated by two asterisks (**$p < 0.01$).

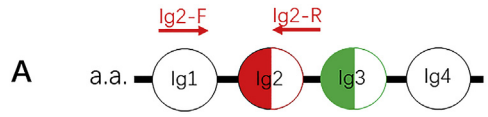


B

| Ig2 | | | | | | | | |
|---|---|---|---|---|---|---|---|---|
| | PBS (100) | | | *EsB52* siRNA (100) | | | *GFP siRNA* (100) | |
| S. | Vi. | N. | S. | Vi. | N. | S. | Vi. | N. |
| 1 | 4-2 | 8 | 1 | 4-2 | 3 | 1 | 4-2 | 5 |
| 2 | 4-3 | 4 | 2 | 4-3 | 7 | 2 | 4-3 | 5 |
| 3 | 4-4 | 3 | 3 | 4-4 | 6 | 3 | 4-4 | 10 |
| 4 | 4-5 | 3 | 4 | 4-5 | 6 | 4 | 4-8 | 3 |
| 5 | 4-8 | 9 | 5 | 4-8 | 4 | 5 | 4-10 | 7 |
| 6 | 4-10 | 10 | 6 | 4-10 | 3 | 6 | 4-12 | 9 |
| 7 | 4-12 | 2 | 7 | 4-12 | 9 | 7 | 4-13 | 9 |
| 8 | 4-13 | 5 | 8 | 4-13 | 8 | 8 | 4-16 | 8 |
| 9 | 4-16 | 5 | 9 | 4-16 | 7 | 9 | 4-17 | 6 |
| 10 | 4-17 | 7 | 10 | 4-17 | 14 | 10 | 4-18 | 9 |
| 11 | 4-18 | 1 | 11 | 4-18 | 3 | 11 | 4-22 | 6 |
| 12 | 4-19 | 6 | 12 | 4-19 | 9 | 12 | 4-23 | 2 |
| 13 | 4-22 | 12 | 13 | 4-22 | 2 | 13 | 4-27 | 5 |
| 14 | 4-23 | 9 | 14 | 4-23 | 6 | 14 | 4-28 | 7 |
| 15 | 4-25 | 10 | 15 | 4-29 | 4 | 15 | 4-29 | 4 |
| 16 | 4-29 | 3 | 16 | 4-31 | 9 | 16 | 4-31 | 5 |
| 17 | 4-31 | 3 | | | | | | |

**Fig. 9. Influence of *EsB52* RNAi on *EsDscam* Ig2 domain.** (A) Specific primers were designed to amplify the Ig2 domain. (B) Ig2 variability was investigated by cloning and sequencing 100 clones from each group (the *EsB52* siRNA experimental, and PBS and *GFP* siRNA control groups). S, serial number; Vi, variable isoforms (Vi numbers were obtained from our previous unpublished studies); N, number of clones.

### 3.4. Expression of EsB52 in hemocytes following immune stimulation

Temporal expression patterns of *EsB52* were determined in hemocytes using RT-qPCR following stimulation with *V. parahaemolyticus*, *S. aureus*, LPS and PG (with *β-actin* as an internal control). Expression of *EsB52* was upregulated significantly upon exposure to *V. parahaemolyticus* (a Gram-negative bacterium) at 24 h (*$p < 0.05$), 36 h (**$p < 0.01$) and 48 h (**$p < 0.01$) after stimulation, peaking up to 7-

A

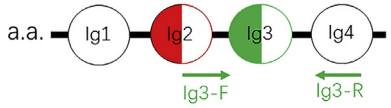


B

| Ig3 | | | | | | | | |
|---|---|---|---|---|---|---|---|---|
| PBS (100) | | | *EsB52* siRNA (100) | | | *GFP* siRNA (100) | | |
| S. | Vi. | N. | S. | Vi. | N. | S. | Vi. | N. |
| 1 | 6-2 | 8 | 1 | 6-2 | 6 | 1 | 6-2 | 2 |
| 2 | 6-3 | 5 | 2 | 6-3 | 8 | 2 | 6-3 | 9 |
| 3 | 6-4 | 3 | 3 | 6-4 | 5 | 3 | 6-4 | 4 |
| 4 | 6-6 | 6 | 4 | 6-8 | 8 | 4 | 6-6 | 9 |
| 5 | 6-10 | 9 | 5 | 6-9 | 6 | 5 | 6-8 | 6 |
| 6 | 6-15 | 5 | 6 | 6-10 | 3 | 6 | 6-9 | 3 |
| 7 | 6-16 | 6 | 7 | 6-15 | 5 | 7 | 6-10 | 3 |
| 8 | 6-19 | 3 | 8 | 6-16 | 9 | 8 | 6-14 | 10 |
| 9 | 6-23 | 4 | 9 | 6-19 | 5 | 9 | 6-15 | 3 |
| 10 | 6-24 | 10 | 10 | 6-23 | 3 | 10 | 6-16 | 5 |
| 11 | 6-26 | 8 | 11 | 6-24 | 1 | 11 | 6-19 | 4 |
| 12 | 6-28 | 7 | 12 | 6-26 | 9 | 12 | 6-23 | 2 |
| 13 | 6-29 | 6 | 13 | 6-28 | 3 | 13 | 6-26 | 6 |
| 14 | 6-30 | 5 | 14 | 6-29 | 4 | 14 | 6-28 | 9 |
| 15 | 6-32 | 6 | 15 | 6-30 | 8 | 15 | 6-29 | 7 |
| 16 | 6-36 | 9 | 16 | 6-35 | 7 | 16 | 6-30 | 7 |
| | | | 17 | 6-36 | 10 | 17 | 6-32 | 5 |
| | | | | | | 18 | 6-35 | 6 |

**Fig. 10. Influence of *EsB52* RNAi on *EsDscam* Ig3 domain**. (A) Specific primers were designed to amplify the Ig3 domain. (B) Ig3 variability was investigated by cloning and sequencing 100 clones from each group (as described in Fig. 9).

A


B

| Ig7 | | | | | | | | |
|---|---|---|---|---|---|---|---|---|
| PBS (100) | | | *EsB52* siRNA (100) | | | *GFP* siRNA (100) | | |
| S. | Vi. | N. | S. | Vi. | N. | S. | Vi. | N. |
| 1 | 14-2 | 21 | 1 | 14-5 | 31 | 1 | 14-2 | 16 |
| 2 | 14-5 | 12 | 2 | 14-10 | 27 | 2 | 14-5 | 9 |
| 3 | 14-9 | 15 | 3 | 14-13 | 7 | 3 | 14-9 | 11 |
| 4 | 14-10 | 9 | 4 | 14-19 | 35 | 4 | 14-10 | 8 |
| 5 | 14-13 | 12 | | | | 5 | 14-11 | 11 |
| 6 | 14-15 | 4 | | | | 6 | 14-13 | 9 |
| 7 | 14-18 | 11 | | | | 7 | 14-15 | 4 |
| 8 | 14-19 | 16 | | | | 8 | 14-18 | 17 |
| | | | | | | 9 | 14-19 | 15 |

**Fig. 11. *EsB52* RNAi decreases the variability of the *EsDscam* Ig7 domain**. (A) Specific primers were designed to amplify the Ig7 domain. (B) Ig7 variability was investigated by cloning and sequencing 100 clones from each group (as described in Fig. 9).

fold at 36 h after stimulation (Fig. 7A). Upon exposure to the Gram-positive *S. aureus*, expression of *EsB52* was also increased significantly (**$p < 0.01$) at 12, 24 and 36 h, peaking up to 9.8-fold at 24 h (Fig. 7B). In response to LPS, *EsB52* was rapidly upregulated, peaking up to 8-fold at 24 h, then dropping at 36 and 48 h (Fig. 7C). *EsB52* was upregulated significantly after PG challenge, peaking up to 5.8-fold at 12 h, then decreasing but remaining above controls at 24 h (Fig. 7D). As expected, there was no significant variation in expression levels in control groups (white bars in Fig. 7A – D).

### 3.5. RNAi silencing of EsB52 in vitro

To investigate the possible regulatory function of *EsB52* targeting on *EsDscam-hv* alternative splicing events, *EsB52* siRNA was transfected into hemocytes, and at 24 h after transfection, qRT-PCR was performed to measure *EsB52* mRNA levels. The expression level of PBS and GFP transfected groups showed no significant different, but both were significant higher than *EsB52* siRNA treated group, which means *EsB52* siRNA suppressed the expression of *EsB52* efficiently (Fig. 8), and this siRNA can be used in the subsequent experiment.

### 3.6. Influence of EsB52 RNAi on EsDscam extracellular hypervariable regions

In order to validate whether *EsB52* is involved in alternative splicing events for *EsDscam*, and if so, how it acts on the three extracellular hypervariable regions (Ig2, Ig3 and Ig7) of *EsDscam*, three pairs of specific primers were designed (Figs. 9A, 10A and 11A) to amplify mRNA from each region. Approximately 100 clones of each region were picked and sequenced, and the results are shown in Figs. 9B, 10B and 11B. The number of exon variants in Ig2 and Ig3 regions following *EsB52* silencing was similar to control (PBS and GFP siRNA) groups (Figs. 9B and 10B), suggesting that *EsB52* RNAi only slightly affected the number of Ig2 and Ig3 isoforms. Therefore, we concluded that *EsB52* is not essential for alternative splicing of Ig2 and Ig3 domains in *EsDscam*.

Comparison of exon variants in Ig7 (Fig. 11B) revealed obvious differences in Ig7 variant populations between *EsB52* silencing and control groups. There were seven and six exon variants in PBS and GFP siRNA groups, respectively, pared with only three variants in the *EsB52* RNAi silencing group, hence *EsB52* RNAi decreased the number of Ig7 variants. Therefore, we concluded that *EsB52* may activate Ig7 alternative splicing.

## 4. Discussion

Decades of genetic and biochemical experiments have identified almost all proteins in the spliceosomes of some organisms, and various functions have been uncovered. However, the structure remained a mystery for a long time, until two parallel research articles [33,34] settled this issue by determining the long-sought-after structure of a yeast spliceosome, which shed light on the molecular mechanism of pre-messenger RNA splicing. In addition to the basic biological importance of the spliceosome, numerous diseases are related to dysfunctional spliceosomal regulation or splicing mistakes. Almost 35% of genetic disorders are the result of incorrect splicing, exemplified by unusual expression of alternative splice variants that leads to frontotemporal dementia driven by tau mis-splicing. The mutation of key spliceosomal proteins such as Brr2 or Prp8 can lead to the autosomal dominant retinitis pigmentosa, and some cancers are associated with abnormal splicing.

The *EsDscam-hv* gene has a similar organisation to its homologs in insects; exons coding for half of Ig domains 2 and 3, and the entire Ig7 domain, are constructed from multiple exons [4]. The *Dscam-hv* gene is an extreme example of alternative splicing that contains more than two mutually exclusive exons [35]. Herein, we identified the docking site (78.4% similarity with *Drosophila*), selector sequences (50–70% identity with docking sites) and the LCR, representing three classes of conserved sequence elements within the *EsDscam-hv* exon 6 cluster that have the potential to engage in base-pairing interactions. The mutually exclusive nature of the interactions of the selector sequences with the docking site suggests that the formation of these structures is a central component of the mechanism, which ensures that only one of the exon 6 variants is included [6,7]. The docking site-selector sequence interactions are somewhat reminiscent of those that direct site-specific RNA editing [36]. An intriguing possibility is that the interaction juxtaposes the exon 6 variant with a splicing regulatory element upstream of the docking site [7].

Interestingly, an additional highly conserved sequence element is located immediately adjacent to the docking site, which is predicted to form a 37 bp stem-loop structure that is supported by multiple compensatory mutations, termed the LCR. Long-range activation of *Dscam-hv* splicing is controlled by LCRs under intense purifying selection. One intronic element upstream of the docking site may have undergone purifying selection and could form the ancestral monomer structure.

Such a structural subunit could act as an LCR to activate the inclusion of the proximal exon when the docking site interacts with a selection sequence [8].

*B52* is a classical SR protein, members of which have one or two RRMs in the N-terminal region and an extensive RS domain in the C-terminal region. As a homolog of human *SRp55*, *B52* is highly conserved across vertebrates and invertebrates, as demonstrated by sequence alignment and phylogenetic analysis [37,38]. The RRMs and RS domain bind to the RNA specifically and promote spliceosome assembly [39]. In the present study, we cloned and characterised the full-length cDNA sequence of *EsB52*, which as the typical domain architecture of other *B52* orthologs (Figs. 3 and 4A). RRM motifs in *EsB52* consist of 60–70 residues and contain two degenerate short submotifs, the RNP-1 octamer and the RNP2 hexamer. In *Drosophila*, *B52* is expressed during all stages of development, indicating its overall importance [37]. Our current results showed that *EsB52* was highly expressed in all tested tissues, especially in brain and hemocytes (Fig. 6). Thus, *EsB52* is an SR protein and *B52* homolog that promotes exon inclusion by acting as a splicing activator.

There are two immune systems that guard against invasion of pathogens; innate immunity and adaptive immunity. Innate immunity occurs in all animals, while adaptive immunity, which has immunological memory, was thought to exist only in vertebrates [40,41]. However, arthropods were so found to exhibit highly specific immune responses against specific pathogens after following identical pathogen challenge [42–45]. Thus, vaccine-like treatments are required for arthropods to guard against the 'conversant' pathogen [45,46]. If invertebrates can recognise different pathogens specifically, their pathogen-specific receptors should display high diversity. In *Drosophila melanogaster*, *Dscam* can generate tens of thousands of isoforms via alternative splicing [5]. In addition, it is noteworthy that arthropods have a large diversified Chelicerata-specific repertoire of nonclassical *Dscam* isoforms, they can enhance protein diversity via alternative promoters [47,48]. *Dscam* is extensively expressed in fat body cells and hemocytes, which are major tissues of the insect immune system, and the immune function of *Dscam* was confirmed by observing its participation in bacterial recognition and phagocytosis [1,11]. Hemocytes are vitally important cells of the invertebrate immune system [49]. In the present study, expression of *EsB52* was upregulated significantly in hemocytes following stimulation by PAMPs and bacteria (Fig. 7A − D). Moreover, *Dscam* transcription was induced after different types of PAMP challenge in Chinese mitten crab [26], and WSSV induced upregulation of *Dscam* and *B52* in shrimp [24]. These findings suggest that following upregulation of *Dscam*, upregulation of *B52* could promote alternative splicing of *Dscam*.

After RNAi silencing of *EsB52* in crab hemocytes, we observed only a slight change in the number of Ig2 and Ig3 isoforms (Figs. 9B and 10B). However, it is too early to conclude that *EsB52* is not involved in *EsDscam* alternative splicing, because *EsDscam* also has other variable regions, and animal physiology is complex. In *Drosophila*, a similar situation has been described, and *B52* is an essential factor in larval development [37,50]. It is possible that other SR proteins can functionally replace *B52* [37]. By contrast, in *EsB52*-silenced crabs, there was a decrease in the number of Ig7 isoforms relative to controls (Fig. 11B), and similar results were described in shrimp [24]. These results indicate that *EsB52* may be involved in *EsDscam* Ig7 alternative splicing.

To conclude, we identified and characterised gene sequences and structures of *EsB52*. *EsB52* was found to be highly expressed in brain and hemocytes, and upregulated significantly following stimulation by PAMPs and bacteria. Thus, *EsB52* acts as a splicing activator of *EsDscam* in *E. sinensis*.

## Acknowledgements

This work was supported by grants from the National Natural Science Foundation of China (31602189 and 31672639), the Modern Fisheries Industry Technology System Project of Jiangsu Province (grant number JFRS-01), the Shanghai Collaborative Innovation Center for Aquatic Animal Genetics and Breeding, the Opening Project of the Key Laboratory of Freshwater Fishery Germplasm Resources, the Ministry of Agriculture, P. R. China, and the Shanghai University Knowledge Service Platform, Shanghai Ocean University Aquatic Animal Breeding Center (ZF1206).

## Appendix A. Supplementary data

Supplementary data to this article can be found online at https://doi.org/10.1016/j.fsi.2019.01.027.

## References

[1] F.L. Watson, R. Puttmann-Holgado, F. Thomas, D.L. Lamar, M. Hughes, M. Kondo, V.I. Rebel, D. Schmucker, Extensive diversity of Ig-superfamily proteins in the immune system of insects, Science 309 (5742) (2005) 1874–1878.
[2] D. Schmucker, B. Chen, Dscam and DSCAM: complex genes in simple animals, complex animals yet simple genes, Genes Dev. 23 (2) (2009) 147–156.
[3] C. Lee, N. Kim, M. Roy, B.R. Graveley, Massive expansions of Dscam splicing diversity via staggered homologous recombination during arthropod evolution, RNA 16 (1) (2010) 91–105.
[4] D. Brites, S. McTaggart, K. Morris, J. Anderson, K. Thomas, I. Colson, T. Fabbro, T.J. Little, D. Ebert, L. Du Pasquier, The Dscam homologue of the crustacean Daphnia is diversified by alternative splicing like in insects, Mol. Biol. Evol. 25 (7) (2008) 1429–1439.
[5] D. Schmucker, J.C. Clemens, H. Shu, C.A. Worby, J. Xiao, M. Muda, J.E. Dixon, S.L. Zipursky, Drosophila Dscam is an axon guidance receptor exhibiting extraordinary molecular diversity, Cell 101 (6) (2000) 671–684.
[6] G. Neves, J. Zucker, M. Daly, A. Chess, Stochastic yet biased expression of multiple Dscam splice variants by individual cells, Nat. Genet. 36 (3) (2004) 240–246.
[7] B.R. Graveley, Mutually exclusive splicing of the insect Dscam pre-mRNA directed by competing intronic RNA secondary structures, Cell 123 (1) (2005) 65–73.
[8] X. Wang, G. Li, Y. Yang, W. Wang, W. Zhang, H. Pan, P. Zhang, Y. Yue, H. Lin, B. Liu, J. Bi, F. Shi, J. Mao, Y. Meng, L. Zhan, Y. Jin, An RNA architectural locus control region involved in Dscam mutually exclusive splicing, Nat. Commun. 3 (2012) 1255.
[9] B.R. Graveley, A. Kaur, D. Gunning, S.L. Zipursky, L. Rowen, J.C. Clemens, The organization and evolution of the dipteran and hymenopteran Down syndrome cell adhesion molecule (Dscam) genes, RNA 10 (10) (2004) 1499–1506.
[10] P.H. Chou, H.S. Chang, I.T. Chen, H.Y. Lin, Y.M. Chen, H.L. Yang, K.C. Wang, The putative invertebrate adaptive immune protein Litopenaeus vannamei Dscam (LvDscam) is the first reported Dscam to lack a transmembrane domain and cytoplasmic tail, Dev. Comp. Immunol. 33 (12) (2009) 1258–1267.
[11] Y. Dong, H.E. Taylor, G. Dimopoulos, AgDscam, a hypervariable immunoglobulin domain-containing receptor of the Anopheles gambiae innate immune system, PLoS Biol. 4 (7) (2006) e229.
[12] A.J. Matlin, F. Clark, C.W. Smith, Understanding alternative splicing: towards a cellular code, Nat. Rev. Mol. Cell Biol. 6 (5) (2005) 386–398.
[13] M. Chen, J.L. Manley, Mechanisms of alternative splicing regulation: insights from molecular and genomics approaches, Nat. Rev. Mol. Cell Biol. 10 (11) (2009) 741–754.
[14] T.W. Nilsen, B.R. Graveley, Expansion of the eukaryotic proteome by alternative splicing, Nature 463 (7280) (2010) 457–463.
[15] E.T. Wang, R. Sandberg, S. Luo, I. Khrebtukova, L. Zhang, C. Mayr, S.F. Kingsmore, G.P. Schroth, C.B. Burge, Alternative isoform regulation in human tissue transcriptomes, Nature 456 (7221) (2008) 470–476.
[16] B. Modrek, C. Lee, A genomic view of alternative splicing, Nat. Genet. 30 (1) (2002) 13–19.
[17] Y. Ding, C.E. Lawrence, A statistical sampling algorithm for RNA secondary structure prediction, Nucleic Acids Res. 31 (24) (2003) 7280–7301.
[18] Y. Yang, L. Zhan, W. Zhang, F. Sun, W. Wang, N. Tian, J. Bi, H. Wang, D. Shi, Y. Jiang, Y. Zhang, Y. Jin, RNA secondary structure in mutually exclusive splicing, Nat. Struct. Mol. Biol. 18 (2) (2011) 159–168.
[19] E.C. Ibrahim, T.D. Schaal, K.J. Hertel, R. Reed, T. Maniatis, Serine/arginine-rich protein-dependent suppression of exon skipping by exonic splicing enhancers, Proc. Natl. Acad. Sci. U. S. A 102 (14) (2005) 5002–5007.
[20] R. Martinez-Contreras, P. Cloutier, L. Shkreta, J.F. Fisette, T. Revil, B. Chabot, hnRNP proteins and splicing control, Adv. Exp. Med. Biol. 623 (2007) 123–147.
[21] S. Olson, M. Blanchette, J. Park, Y. Savva, G.W. Yeo, J.M. Yeakley, D.C. Rio, B.R. Graveley, A regulator of Dscam mutually exclusive splicing fidelity, Nat. Struct. Mol. Biol. 14 (12) (2007) 1134–1140.
[22] J.W. Park, K. Parisky, A.M. Celotto, R.A. Reenan, B.R. Graveley, Identification of alternative splicing regulators by RNA interference in Drosophila, Proc. Natl. Acad. Sci. U. S. A 101 (45) (2004) 15974–15979.
[23] D.T. Champlin, M. Frasch, H. Saumweber, J.T. Lis, Characterization of a Drosophila protein associated with boundaries of transcriptionally active chromatin, Genes Dev. 5 (9) (1991) 1611–1621.
[24] Y.A. Chiang, H.Y. Hung, C.W. Lee, Y.T. Huang, H.C. Wang, Shrimp Dscam and its

cytoplasmic tail splicing activator serine/arginine (SR)-rich protein B52 were both induced after white spot syndrome virus challenge, Fish Shellfish Immunol. 34 (1) (2013) 209–219.
[25] D. Hattori, S.S. Millard, W.M. Wojtowicz, S.L. Zipursky, Dscam-mediated cell recognition regulates neural circuit formation, Annu. Rev. Cell Dev. Biol. 24 (2008) 597–620.
[26] X.K. Jin, W.W. Li, M.H. Wu, X.N. Guo, S. Li, A.Q. Yu, Y.T. Zhu, L. He, Q. Wang, Immunoglobulin superfamily protein Dscam exhibited molecular diversity by alternative splicing in hemocytes of crustacean, Eriocheir sinensis, Fish Shellfish Immunol. 35 (3) (2013) 900–909.
[27] S. Schwartz, Z. Zhang, K.A. Frazer, A. Smit, C. Riemer, J. Bouck, R. Gibbs, R. Hardison, W. Miller, PipMaker–a web server for aligning two genomic DNA sequences, Genome Res. 10 (4) (2000) 577–586.
[28] G.E. Crooks, G. Hon, J.M. Chandonia, S.E. Brenner, WebLogo: a sequence logo generator, Genome Res. 14 (6) (2004) 1188–1190.
[29] M. Zuker, Mfold web server for nucleic acid folding and hybridization prediction, Nucleic Acids Res. 31 (13) (2003) 3406–3415.
[30] V.J. Smith, K. Soderhall, Induction of degranulation and lysis of haemocytes in the freshwater crayfish, Astacus astacus by components of the prophenoloxidase activating system in vitro, Cell Tissue Res. 233 (2) (1983) 295–303.
[31] K.J. Livak, T.D. Schmittgen, Analysis of relative gene expression data using real-time quantitative PCR and the 2(-Delta Delta C(T)) Method, Methods 25 (4) (2001) 402–408.
[32] Y.T. Zhu, D. Li, X. Zhang, X.J. Li, W.W. Li, Q. Wang, Role of transglutaminase in immune defense against bacterial pathogens via regulation of antimicrobial peptides, Dev. Comp. Immunol. 55 (2016) 39–50.
[33] J. Hang, R. Wan, C. Yan, Y. Shi, Structural basis of pre-mRNA splicing, Science 349 (6253) (2015) 1191–1198.
[34] C. Yan, J. Hang, R. Wan, M. Huang, C.C. Wong, Y. Shi, Structure of a yeast spliceosome at 3.6-angstrom resolution, Science 349 (6253) (2015) 1182–1191.
[35] G.E. May, S. Olson, C.J. McManus, B.R. Graveley, Competing RNA secondary structures are required for mutually exclusive splicing of the Dscam exon 6 cluster, RNA 17 (2) (2011) 222–229.
[36] R.A. Reenan, The RNA world meets behavior: A– > I pre-mRNA editing in animals, Trends Genet. : TIG (Trends Genet.) 17 (2) (2001) 53–56.
[37] B.E. Hoffman, J.T. Lis, Pre-mRNA splicing by the essential Drosophila protein B52: tissue and target specificity, Mol. Cell Biol. 20 (1) (2000) 181–186.
[38] A.M. Zahler, W.S. Lane, J.A. Stolk, M.B. Roth, SR proteins: a conserved family of pre-mRNA splicing factors, Genes Dev. 6 (5) (1992) 837–847.
[39] J.C. Long, J.F. Caceres, The SR protein family of splicing factors: master regulators of gene expression, Biochem. J. 417 (1) (2009) 15–27.
[40] M.D. Cooper, M.N. Alder, The evolution of adaptive immune systems, Cell 124 (4) (2006) 815–822.
[41] A.F. Rowley, A. Powell, Invertebrate immune systems specific, quasi-specific, or nonspecific? J. Immunol. (Baltimore, Md.: 1950) 179 (11) (2007) 7209–7214.
[42] J. Kurtz, K. Franz, Innate defence: evidence for memory in invertebrate immunity, Nature 425 (6953) (2003) 37–38.
[43] B.M. Sadd, P. Schmid-Hempel, Insect immunity shows specificity in protection upon secondary pathogen exposure, Curr. Biol. : CB 16 (12) (2006) 1206–1210.
[44] L.N. Pham, M.S. Dionne, M. Shirasu-Hiza, D.S. Schneider, A specific primed immune response in Drosophila is dependent on phagocytes, PLoS Pathog. 3 (3) (2007) e26.
[45] A. Powell, E.C. Pope, F.E. Eddy, E.C. Roberts, R.J. Shields, M.J. Francis, P. Smith, S. Topps, J. Reid, A.F. Rowley, Enhanced immune defences in Pacific white shrimp (Litopenaeus vannamei) post-exposure to a vibrio vaccine, J. Invertebr. Pathol. 107 (2) (2011) 95–99.
[46] K.N. Johnson, M.C. van Hulten, A.C. Barnes, "Vaccination" of shrimp against viral pathogens: phenomenology and underlying mechanisms, Vaccine 26 (38) (2008) 4885–4892.
[47] G. Cao, Y. Shi, J. Zhang, H. Ma, S. Hou, H. Dong, W. Hong, S. Chen, H. Li, Y. Wu, P. Guo, X. Shao, B. Xu, F. Shi, Y. Meng, Y. Jin, A chelicerate-specific burst of nonclassical Dscam diversity, BMC Genomics 19 (1) (2018) 66.
[48] Y. Yue, Y. Meng, H. Ma, S. Hou, G. Cao, W. Hong, Y. Shi, P. Guo, B. Liu, F. Shi, Y. Yang, Y. Jin, A large family of Dscam genes with tandemly arrayed 5' cassettes in Chelicerata, Nat. Commun. 7 (2016) 11252.
[49] X. Lin, I. Soderhall, Crustacean hematopoiesis and the astakine cytokines, Blood 117 (24) (2011) 6417–6424.
[50] H.Z. Ring, J.T. Lis, The SR protein B52/SRp55 is essential for Drosophila development, Mol. Cell Biol. 14 (11) (1994) 7499–7506.